Electric double layer effect in the vicinity of solid electrolyte/diamond interfaces and the application to neuromorphic computing

Takashi Tsuchiya[1], Makoto Takayanagi[1,2], Daiki Nishioka[1,2,3], Wataru Namiki[1], and Kazuya Terabe[1]

1. Research Center for Materials Nanoarchitectonics (MANA), National Institute for Materials Science (NIMS), 1-1 Namiki, Tsukuba, Ibaraki 305-0044, Japan
2. Department of Applied Physics, Faculty of Science, Tokyo University of Science, 6-3-1 Niijuku, Katsushika, Tokyo 125-8585, Japan
3. International Center for Young Scientists (ICYS), National Institute for Materials Science (NIMS), Sengen 1-2-1, Tsukuba, Ibaraki 305-0047, Japan

E-mail: TSUCHIYA.Takashi@nims.go.jp

Abstract

Electric double layer effect in solid electrochemical systems is a key topic in energy storage applications. In this review, we outline recent investigations on the electric double layer effect of solid electrolyte interfaces by utilizing a semiconducting diamond surface as a probe of electrical charges at the solid/solid interfaces. Hall measurements with various solid electrolyte-based transistors evidenced that the electric double-layer effect strongly depends on the properties of the electrolyte and the very thin region from the interface. The unveiled features of the electric double layer at solid electrolyte interfaces are quantitatively discussed from the viewpoint of charge density and charging-discharging rate. Furthermore, applications of the unique switching response of the electric double layer transistors to neuromorphic computing are also demonstrated.

1. Introduction

Colossal energy consumption and carbon emissions are becoming a severe problem in many parts of the world, and a shift to electric vehicles is underway to solve the problem. Developing technologies related to electric vehicles is essential, and developing high-power, all-solid-state batteries is particularly urgent. All-solid-state batteries consist entirely of solid materials for electrodes and electrolytes and have advantages over lithium-ion batteries, which use liquid electrolytes in terms of high output and high safety with no risk of ignition, which has led to intensified research competition worldwide.[1] On the other hand, the output of all-solid-state

batteries is currently not sufficiently high, and one of the main reasons for this is the high interface resistance. Various factors have been discussed concerning the high interfacial resistance, among which the interfacial phenomenon known as the electric double-layer effect or space-charge-layer effect has attracted much attention.[2-6] The electric double-layer effect is caused by the distribution of ion concentration inside the electrolyte and electrode,[7] and corresponds to the depletion layer and Schottky barrier in the semiconductor field, which are known to strongly influence the interfacial resistance of the electron current across the electrode/semiconductor interface,[8] and is therefore suggested to have a significant effect on interfacial resistance in all-solid-state batteries as well. It is suggested that they impact the interface resistance in all-solid-state batteries. Several cases have been reported in which the dominant contribution of the electric double layer or space charge layer to the lithium ion transfer resistance at the solid electrolyte/electrode interface is suspected to change the battery output by several orders of magnitude. Investigation of the electric double layer or space charge layer at the solid electrolyte interface is an urgent task.[3-5] However, while the electric double layer or space charge layer has been investigated in great detail in electrochemical systems with liquid electrolytes, it is still at a fundamental stage in electrochemical systems with solid electrolytes and is poorly understood, including its existence. The reason for this lack of understanding of the electric double layer in solid systems is that solid electrolytes tend to be ionic and electronic mixed conductors due to electron conduction caused by internal charge compensation in conjunction with ionic transport,[9-12] and the resulting chemical capacitance complicates the system, making detailed analysis using conventional electrochemical measurements difficult. This is due to the difficulty of detailed analysis by conventional electrochemical measurements. Therefore, new experimental methods that do not rely on conventional methods are needed to investigate the electrochemical double-layer effects in solid electrolyte systems.

We have recently pioneered a novel method to probe the electric double layer effect at the solid electrolyte interface.[13] This method, inspired by the field-effect transistor principle in semiconductor science, utilizes chemically inert diamond as the semiconductor channel material. By creating an ion-blocking interface that hinders ion transfer between the solid electrolyte and semiconductor channel, we were able to quantitatively assess the electric double layer effects occurring at this interface and the modulation behavior induced by applying an external voltage through Hall measurements. These investigations unveiled the existence of the electric double layer effect at the solid electrolyte interface and its strong dependence on the material. We also discovered that the charge-discharge rate of such an electric double layer varies over several orders of magnitude under the dominant influence of the material and composition in the immediate vicinity of the solid electrolyte/semiconductor

channel interface.[14] Moreover, we have recently demonstrated the application of electric double-layer transistors using solid electrolytes in high-efficiency information processing, specifically neuromorphic computing, a burgeoning field in electrical information, with exceptional performance.[14-16] This article presents the recent strides in our fundamental and applied research on the electric double-layer effect near the solid electrolyte interface.

2. Evaluation of electric double layer charge near various solid electrolyte/diamond interfaces.

This study utilized the field-effect transistor (FET) operation mechanism usually used in electronic circuits built into electronic products.[8] FET has a structure in which a dielectric oxide thin film (e.g., SiO_2, Al_2O_3) is inserted between a gate electrode and a semiconductor channel (e.g., p-Si, n-Si).[8] Application of a voltage between gate and source electrodes (i.e., gate voltage, V_G) injects an electric charge on the surface of the semiconductor channel, resulting in the wide modulation of the electronic carrier density (e.g., electron, hole) and controlling the electronic current between the source and drain electrodes (i.e., semiconductor channel).[8] Whereas insulators without a trace of ion conduction are used for the dielectric part of FETs in conventional electronic circuits, a lithium solid electrolyte thin film was used for the dielectric part of the FET in this study. Furthermore, an ion-blocking property of diamond, in which lithium ions do not react, was employed for the semiconductor part.[17,18] Thanks to the FET structure, we can selectively detect electric double layer charges on the surface of the electrode (semiconductor channel) formed in the electric double-layer mechanism with various solid electrolytes. First, we investigated the electric double layer effect using two different Li+ solid electrolytes, Li-Si-Zr-O (LSZO) and La-Li-Ti-O (LLTO) thin films, which have comparable Li+ conductivity, though the film composition (elements) is different. Both solid electrolyte thin films have an amorphous nature, which was obtained by room temperature deposition via pulsed laser deposition method with a UV excimer laser (a wavelength of 193 nm). We fabricated three transistors termed LSZO, LLTO, and LLTO/LSZO transistors, as shown in Fig.1, on the surface of the flat surface of a hydrogen-terminated diamond single crystal with lithography patterned electrodes. While LSZO and LLTO transistors are diamond-based transistors with LSZO or LLTO films, LLTO/LSZO transistor is LSZO transistor with a 5 nm LLTO interlayer inserted at the diamond/LSZO interface, meaning that the Li^+ electrolyte at the interface is not LSZO but LLTO.

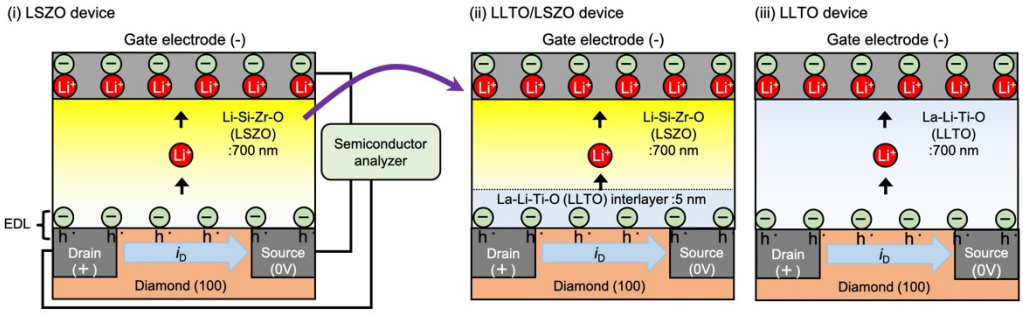

Fig. 1. Illustrations of three diamond-based electric double layer transistors consisted of LSZO or LLTO Li^+ solid electrolyte thin films.[13] Reproduced from [13] by The Author(s) licensed under CC BY 4.0, published by Springer Nature.

Figure 2 shows the V_G dependence of the hole density measured by Hall measurements.[13] The V_G polarity is positive in that Li^+ are removed more out of the hydrogen-terminated diamond/Li^+ solid electrolyte interface. As the V_G is increased in the positive polarity, the hole density on the diamond surface changes by about three orders of magnitude from 4×10^{10} cm^{-2} to 2×10^{13} cm^{-2} due to the electric double layer effect in the LSZO transistor. The result evidenced that electric double layer effect exists even with a solid electrolyte system. In contrast to the LSZO transistor, the LLTO transistor showed no change in the hole density in the V_G range. In addition, the LLTO/LSZO transistor with a 5 nm thick LLTO interlayer also showed very slight carrier density changes similar to the LLTO transistor. The clear difference between the two groups, one is LSZO transistor, and the other is LLTO and LLTO/LSZO transistors, indicates that the electric double layer effect accompanied by hole density modulation is hindered at the LLTO thin film interface, in contrast to the LSZO thin film interface. These results further indicate that the property of electric double layer at the solid electrolyte interface is strongly influenced by the electrolyte composition in a very thin region from the semiconductor/solid electrolyte interface.

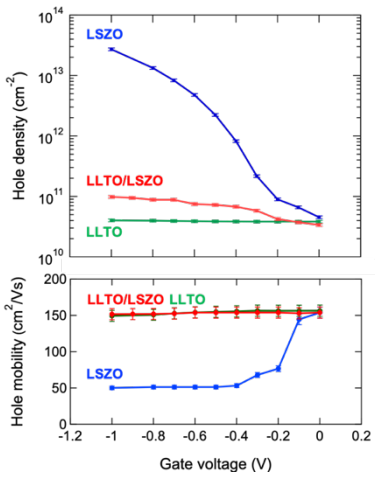

Fig. 2. V_G dependence of hole density and mobility for LSZO, LLTO and LLTO/LSZO transistors.[13] Reproduced from [13] by The Author(s) licensed under CC BY 4.0, published by Springer Nature.

To investigate the origin of the suppression of the electric double layer effect of the LLTO thin film observed in the Hall measurement of **Fig. 2**, in situ scanning transmission electron microscopy electron energy-loss spectroscopy (STEM-EELS) observations were carried out.[13] A two-terminal cell with a diamond electrode/LLTO thin film (5 nm)/LSZO thin film/$LiCoO_2$ electrode shown in **Fig. 3(a)** was fabricated, and the Li *K*-edge and Ti *L*-edge EEL spectra near the diamond electrode/LLTO thin film interface were measured while applying a DC voltage. The voltage direction is positive in that lithium ions are drawn more from the diamond/solid electrolyte interface. The depth profiles of lithium ions obtained using the integrated intensity of the Li *K*-edge EEL spectra are shown in **Fig. 3(b)**. At the LLTO/LSZO interface, Li^+ transfer/transport is driven by a gradient of electrochemical potential of Li^+, $\tilde{\mu}_{Li^+} = \mu_{Li^+} + F\emptyset$ until $\tilde{\mu}_{Li^+}$ for the LLTO thin film ($\tilde{\mu}_{Li^+,LLTO}$) becomes equal to the one for LSZO thin film ($\tilde{\mu}_{Li^+,LSZO}$). Even under the condition that there is no $\emptyset$ gradient due to V=0V and thus $\mu_{Li^+,LLTO} = \mu_{Li^+,LSZO}$, Li^+ concentration ($[Li^+]$) can differ between the LLTO and LSZO layers since $\mu_{Li^+}(= \mu^{\circ}_{Li^+} + RT\ln\gamma_{Li^+} + RT\ln[Li^+])$ includes terms of a standard chemical potential of Li^+ ($\mu^{\circ}_{Li^+}$) and an activity coefficient (γ_{Li^+}), which are unique to LLTO and LSZO respectively. The distribution state of Li ions at V=0 V can be understood in the mechanism. Figure 3(b) shows that the lithium ion concentration in the LLTO and LSZO thin films was significantly lower at V= 1 V compared to the depth profiles at V = 0 V. From this result, it was confirmed that the insertion of LLTO thin film did not hinder the transport of lithium ions and that changes in the concentration of lithium ions occurred.

The Ti *L*-edge EEL spectrum measured in the LLTO thin film region under similar

voltage application conditions is shown in **Fig. 3(c)**: the spectral shape observed at V=0 V consists of the L_2 and L_3 peaks and is in good agreement with the spectral shape widely observed in materials in which the Ti ion shows +4 valence.[19] However, a slight shift towards the low energy loss side is observed due to the contribution of the +3 valence, which is located on the lower energy loss side than the +4 valence. On the other hand, in the spectrum observed at V=1 V, both L_2 and L_3 peaks shifted towards the high energy loss side. This indicates that the excess negative charge generated by the lithium ions being pulled out of the LLTO thin film by applying positive voltage is compensated by the oxidation reaction of Ti ions from +3 to +4 valence. In other words, the suppression of hole density change observed in the hole measurement of the transistor using the LLTO thin film is considered to be caused by the charge compensation by the redox reaction of Ti ions in the LLTO thin film. Therefore, the contrasting differences observed between LSZO and LLTO electrolytes can be understood by considering charge compensation inside the electrolyte.

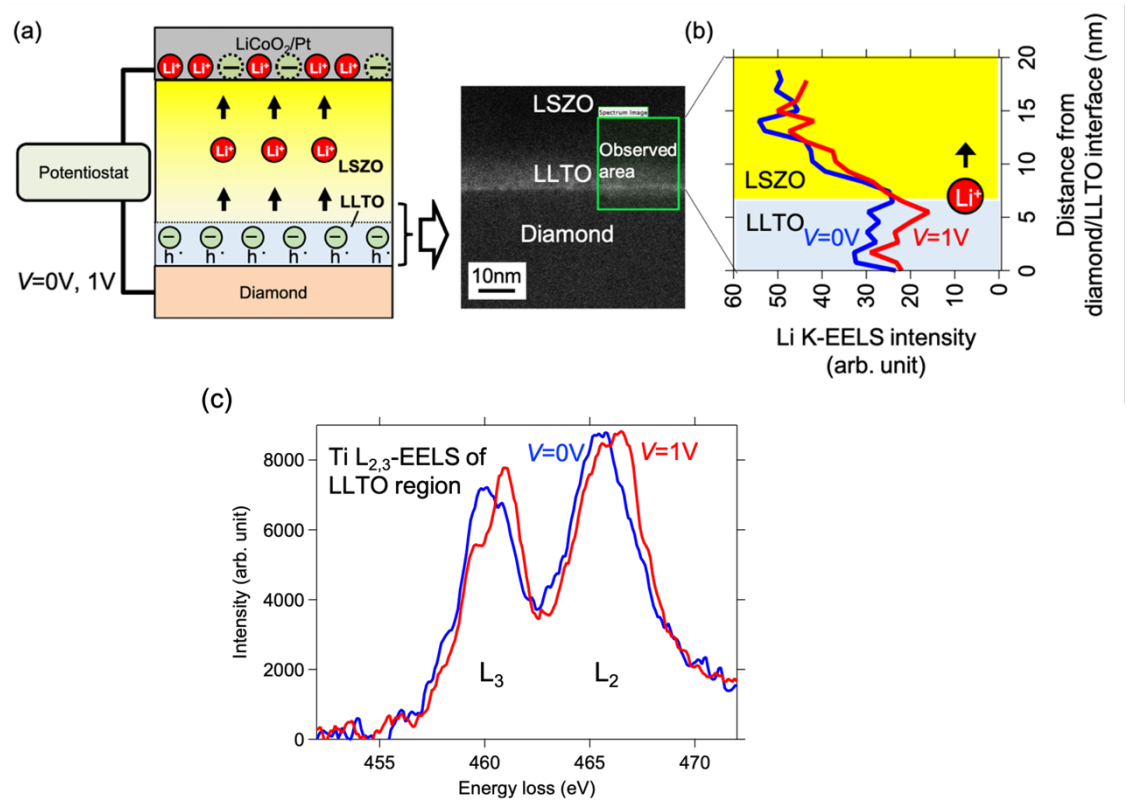

Fig.3 (a) 2-terminal cell for STEM-EELS. (b) depth distribution of lithium ions obtained from Li *K*-edge EEL spectra. (c) Ti *L*-edge EEL spectra measured in the LLTO region.[13] Reproduced from [13] by The Author(s) licensed under CC BY 4.0, published by Springer Nature.

3. Control of electric double layer charge-discharge dynamics by using thin interlayer

The previous section reviewed investigations of electric double layer charges at solid electrolyte interfaces under steady state conditions. The information is useful for discussing the ability of solid electrolytes to form electric double layer charges at the interfaces with a specific electrode or channel material. On the other hand, the investigation mainly done with Hall measurements gives no information on the charging and discharging rate of the electric double layer. In this section, investigations of real-time dynamics of the electric double layer with transistors consisting of various solid electrolytes were done by measuring transient drain current (i_D) response under pulsed V_G applied conditions.

Figure 4(a) shows the i_D transient response of the LSZO transistor measured at various temperatures. The i_D response between i_{ON} and i_{OFF} becomes fast as the temperature rises.[13] The inset of **Fig. 4(a)** shows the definition of the time constant τ of the i_D response as the time for i_D to decrease to 1/e (i.e. 37%) of the initial i_D value. Specifically, τ is 12 ms at 298 K and 490 μs at 340 K. **Figure 4(b)** shows an Arrhenius-type plot of $1/\tau$. The ionic conductivity of the LSZO thin film is also plotted in the figure for comparison. Arrhenius-type thermal activation with an activation energy (E_A) of about 0.657 eV was observed in $1/\tau$ and ionic conductivity. This supports that the ionic conductivity of the LSZO strongly affects the i_D switching response.

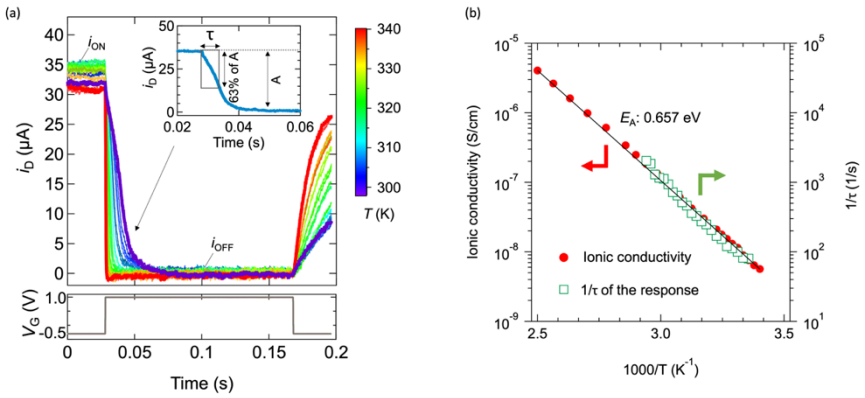

Fig. 4 (a) i_D transient response of the LSZO transistor. (b) Arrhenius-type plot of ionic conductivity of $1/\tau$ and LSZO.[13] Reproduced from [13] by The Author(s) licensed under CC BY 4.0, published by Springer Nature.

We tackled to tune the response by insertion of another two types of Li^+ solid electrolyte at the LSZO/diamond interface of the LSZO transistor.[20] 5 nm thick amorphous $LiNbO_3$ and amorphous Li_3PO_4 films deposited by pulsed laser deposition were inserted at the LSZO/diamond interface as an interlayer. With the transistors, the temperature

dependence of the i_D transient response was measured as shown in the Arrhenius-type plot of $1/\tau$ in Fig. 5.20 The result evidences that the insertion of the thin interlayer has a huge impact on the i_D response speed.[20] Specifically, $1/\tau$ of the $LiNbO_3$ transistor was 4132 (τ = 229 μs) at 298 K, more than ten times faster than the LSZO device (τ = 12.5 ms), while $1/\tau$ of the Li_3PO_4 transistor was 11.6 (τ = 61.4 ms), which is significantly slower than the LSZO transistor. From the above, it is concluded that the $LiNbO_3$ or Li_3PO_4 interlayer has excellent control over the i_D response speed.[20]

An Arrhenius-type plot of $1/\tau$ in LSZO devices with $LiNbO_3$ interlayer of various thicknesses is shown in **Fig. 6.**[20] No notable variation in $1/\tau$ on the thickness of $LiNbO_3$ interlayer was observed when the thickness of the $LiNbO_3$ interlayer was reduced from 5 nm to 1 nm. However, as the thickness of the $LiNbO_3$ interlayer decreased from 1 nm to 1 Å, the i_D transient response rate decreased significantly and asymptotically approached the $1/\tau$ of LSZO devices. In this region, the value of $1/\tau$ and the apparent activation energy depended on the film thickness. These results suggest that the electric double layer's charge-discharge properties are under the electrolyte's dominant influence in the range of about 5 Å from the diamond interface.

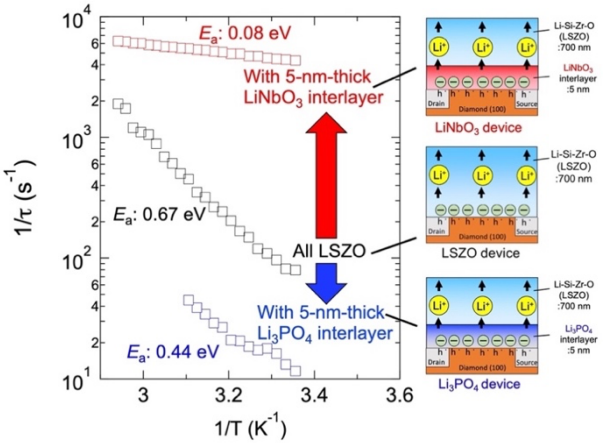

Fig. 5 Arrhenius-type plot of $1/\tau$ for LSZO, $LiNbO_3$, and Li_3PO_4 devices.[20]

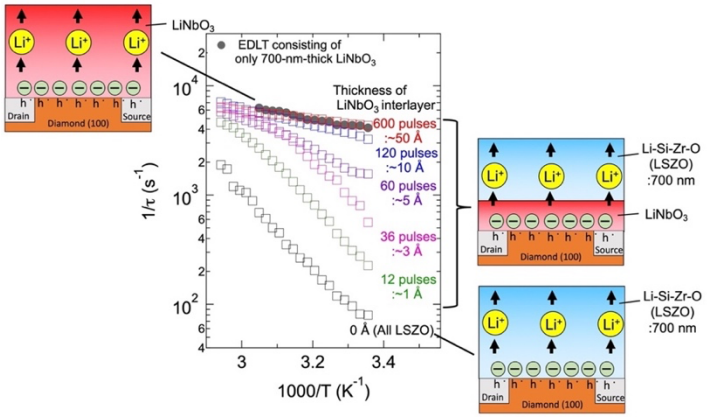

Fig. 6 Variation in $1/\tau$ of $LiNbO_3$ devices with $LiNbO_3$ interlayer of various thicknesses.[20] Copyright © 2023 by Elsevier. Reprinted by permission of Elsevier.

4. Ultrafast charging-discharging dynamics of a porous proton conductor-based solid state electric double layer transistor

The electric double-layer effect has been observed not only in lithium-conducting solid electrolytes but also in proton-conducting solid electrolytes.[14] Nanograined or porous zirconia-based oxides are known to show high proton conductivity.[21-25] Y-stabilized zirconia (YSZ) thin films deposited by pulsed laser deposition at low substrate temperatures have fine nanopores and exhibit high proton conductivity due to the contribution of three types of water molecules (i.e., chemisorbed water, physisorbed water, hydrogen-bonded water) supplying proton conduction paths.[26] A schematic diagram of an electric double-layer transistor using this YSZ film and hydrogen-terminated diamond is shown in **Fig.7**.[14] As in the case of the lithium solid electrolyte, the application of a V_G causes the transport of positively charged protons. It can control the electric double layer at the diamond/solid electrolyte interface. The drain current's response to applying a V_G pulse is shown in **Fig. 8(a)**.[14] Since the observed response is much faster than the other reported EDL devices, there was a doubt whether the response is due to proton conduction of YSZ, or dielectric property of YSZ. The temperature dependence of the relaxation time is shown in **Fig. 8(b)**.[14] In contrast to the case of lithium solid electrolytes, which speed up in the normal Arrhenius-type thermal activation with increasing temperature, a non-Arrhenius-type thermal activation is observed. This is in good agreement with the temperature-dependent character of proton conduction in the porous YSZ thin films,[22,23] supporting that the charge-discharge response of the electric double layer is closely related to the ion transport in the electrolyte regardless of the type of ionic carriers, not related to dielectric property of YSZ.[27,28] A comparison of the relaxation time at room temperature with previously reported electric double-layer transistors is shown in **Fig. 9**.[14]

While standard electric double-layer transistors exhibit a relaxation time of more than 10 ms, the YSZ-type electric double-layer transistor exhibits by far the shortest relaxation time of 27 μs, which is the highest speed of electric double layer transistors reported so far.[13,20,29-32]

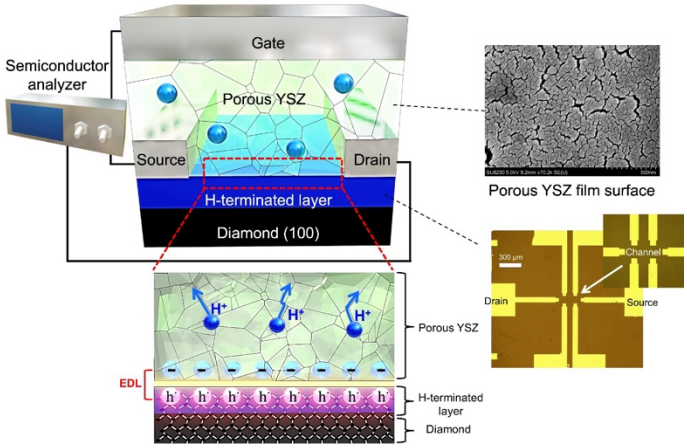

Fig.7 Illustration of hydrogen-terminated diamond-based electric double layer transistor comprised of porous YSZ thin film.[14] Reproduced from [14] by The Author(s) licensed under CC BY 4.0, published by Elsevier.

(a) (b)

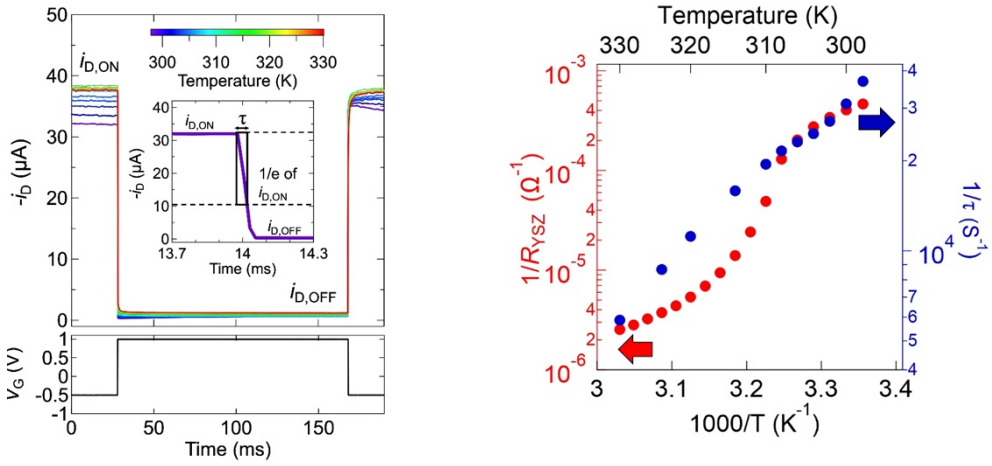

Fig.8(a) The i_d response to applying a V_G pulse. (b) The temperature dependence of the $1/\tau$ and ionic conductivity of YSZ thin film.[14] Reproduced from [14] by The Author(s) licensed under CC BY 4.0, published by Elsevier.

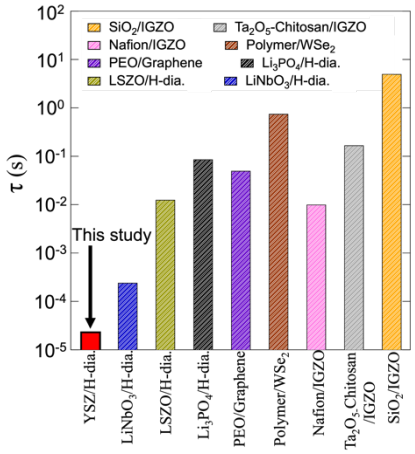

Fig.9 The comparison of τ with electric double layer transistors.[13,14,20,29-32] Reproduced from [14] by The Author(s) licensed under CC BY 4.0, published by Elsevier.

5. Application of solid state electric double layer transistors to neuromorphic computing

Energy consumption due to machine learning, such as deep learning and generative AI, has recently become a serious social problem. To solve this, neuromorphic devices that perform machine learning with high efficiency are needed. Among various methods, reservoir computing, which uses the non-linear responses of dynamical systems as computational resources for neuromorphic computing, has attracted particular attention.[33-38] This method can learn using far fewer computational parameters than general deep learning and thus can achieve low power consumption and high speed. To perform this reservoir computing with high performance, a dynamical system with strong non-linearity is required, and small devices are advantageous for highly integrated implementation in semiconductor devices. We have therefore attempted to apply the previously described solid electrolyte electric double layer transistor to reservoir computing.

Figure 10(a) shows a schematic diagram of an ion-gating reservoir, an electric double layer transistor specially designed for physically implementing reservoir computing.[15] Notable structural difference with typical electric double-layer transistors is that it has many drain electrodes useful for measuring various drain current responses from each semiconductor channel. The different channel lengths vary the transient drain current response. For specific information processing, time-series data is input to the ion-gating reservoir through the common gate electrode as a V_G pulse train, converted from the original time-series data. The applied V_G modifies the charge density of the electric double layer and the drain current, leading to transient drain current dynamics with a quasi-synaptic response featuring sharp

spikes and current relaxation with various speeds, as shown in **Fig. 10(a)**.[15] Despite the relatively simple transistor structure, the device generates such a complex current response. This is because the transport of ions in the electrolyte and the transport of electrons (holes) in the semiconductor channel affect each other near the electric double layer at the diamond/electrolyte interface, which can be termed ion-hole coupled dynamics.[15] The ion-gating reservoir's complex response was useful for performing reservoir computing. The performance was evaluated with a typical benchmark test of reservoir computing termed the 2nd-order nonlinear dynamic equation prediction task, a prediction task of time-series data. **Figure 10(b)** shows a comparison of the target waveform, which was generated by the 2nd-order nonlinear dynamic equation, and the prediction waveform, which was predicted based on the output of the ion-gating.[15] The prediction waveform generated by the ion-gating reservoir precisely reproduced the characteristic features of the target waveform. The ion-gating reservoir achieved the normalized mean square error, an indicator of the prediction performance, which is notably lower than the other reservoir computing devices, including spin torque oscillators and memristors.[39,40] The result evidenced the prominent performance of our ion-gating reservoir. The high performance was found to originate from a feature of the “edge of chaos” as a dynamical system, which is a dynamical state between order and chaos (disorder) and is known to be advantageous for information processing due to its high nonlinearity.[41-44] Similar physical reservoir computing can be performed by YSZ-based electric double layer transistor shown in **Fig. 7**.[14] **Figure 10(c)** shows target and output waveforms for nonlinear transformation task, performed with the YSZ-based ion-gating reservoir (IGR) operating with proton transport.[14] Various target waveforms (sine wave, square wave, phase shift wave, second harmonic wave) were successfully reproduced in the IGR-output waveforms from a triangle wave. The accuracy is higher than other reported physical reservoirs.[42,45] These results indicate a new direction of sold state ionics devices, including electric double layer and redox mechanisms.[46-53]

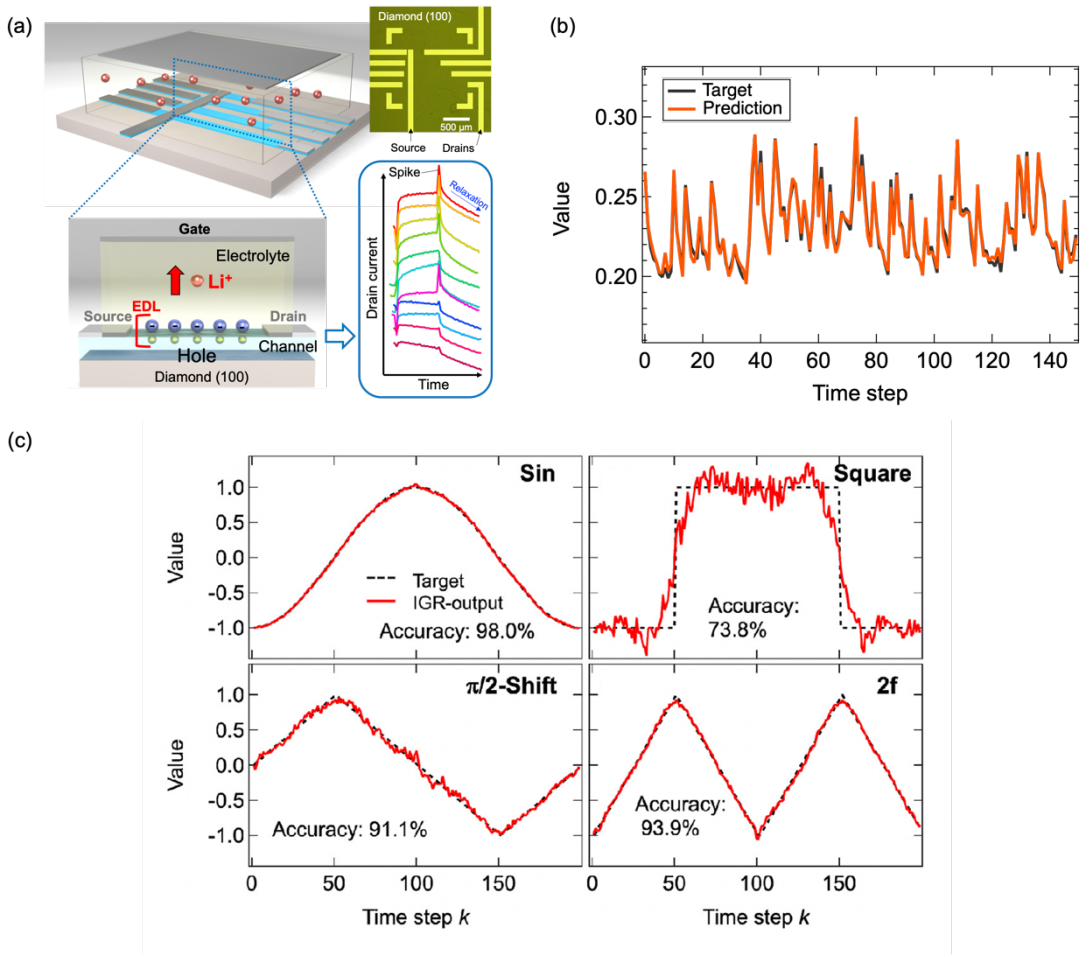

Fig. 10. (a) A schematic diagram of the ion-gating reservoir consisting of hydrogen-terminated diamond and Li^+ solid electrolyte. (b) A comparison with target and prediction waveforms of the benchmark task (2nd-order nonlinear dynamic equation prediction task).[15] Reproduced from [15] by The Author(s) licensed under CC BY-NC 4.0, published by the American Association for the Advancement of Science. (c) A comparison with target and IGR-output waveforms of the nonlinear transformation task.[14] Reproduced from [14] by The Author(s) licensed under CC BY 4.0, published by Elsevier.

6. Conclusion

Field-effect transistors consisting of solid electrolytes and diamonds developed to investigate the electric double-layer effect of solid electrolytes and their application to state-of-the-art neuromorphic computing are outlined. The chemical stability of the diamond makes it suitable for investigating the electric double layer in ion-blocking conditions. Field-effect transistors containing this diamond and lithium solid electrolytes have been prepared, and electrical measurements, such as Hall measurements, have shown that the holes induced on the diamond surface by the electric double-layer effect are high density of around 10^{13} /cm^2

at the interface of lithium solid electrolytes such as LSZO, Li_3PO_4 and $LiNbO_3$, but very low at the interface of LLTO.[13] These results indicate that the electric double-layer effect depends on the properties of the electrolyte; EELS measurements suggest that the suppression of the electric double-layer at the LLTO interface is due to the redox of Ti.[13] Furthermore, the charge-discharge rates of the electric double layer were investigated in detail for several electrolytes, with a difference of more than two orders of magnitude between $LiNbO_3$ and Li_3PO_4.[20] It was suggested that these charge/discharge rates were very strongly influenced by a region of about 5 Å from the diamond surface. Electric double-layer transistors were also prepared using porous YSZ thin films exhibiting high proton conductivity, and the fastest response ever reported was obtained.[14] The transient response of the electric double-layer transistor was applied to reservoir computing, a type of neuromorphic computing, where the complex electrical response due to ion-electron coupled dynamics enables highly accurate time series data prediction tasks.[15] The interface formed by a solid electrolyte is a simple and very small area that can perform various functions such as energy storage and information processing.[54] These interfacial functions not only strongly depend on the properties of the bulk materials and thin films that constitute the interface but also have a high affinity with nanomaterials, including inorganic, organic, and low-dimensional materials designed by the Nanoarchitectonics principle, which has been reported extensively in recent years, and is expected to make dramatic developments based on materials science.[55-60] Establishing basic science on interfacial functions, including the electric double-layer effect, and actively applying it to a wide range of industries is of great importance in solving the severe problems we are facing this century, such as enormous energy consumption and information explosion.

Acknowledgments

This work was in part supported by Japan Society for the Promotion of Science (JSPS) KAKENHI Grant Number JP22H04625 (Grant-in-Aid for Scientific Research on Innovative Areas “Interface Ionics”), and JP22KJ2799 (Grant-in-Aid for JSPS Fellows). A part of this work was supported by JST PRESTO Grant number, JPMJPR23H4. A part of this work was supported by "Advanced Research Infrastructure for Materials and Nanotechnology in Japan (ARIM)" of the Ministry of Education, Culture, Sports, Science and Technology (MEXT) Proposal Number JPMXP1223NM5072, JPMXP1224NM5236 and JPMXP1224NM5237. We are grateful to Prof. Higuchi, Prof. Y. Koide, Dr. M. Imura, Dr. S. Ueda, and Dr. K. Mitsuishi for collaboration on these works.

References

1. K. Takada. Progress in solid electrolytes toward realizing solid-state lithium batteries.

Journal of Power Sources. 394, 74-85(2018).

2. Ohta, N.; Takada, K.; Zhang, L.; Ma, R.; Osada, M.; Sasaki, T. Enhancement of the high-rate capability of solid-state lithium batteries by nanoscale interfacial modification. *Adv. Mater.* **2006**, *18*, 2226-2229.
3. Ohta, N.; Takada, K.; Sakaguchi, L.; Zhang, L.; Ma, R.; Osada, M.; Sasaki, T. $LiNbO_3$-coated $LiCoO_2$ as cathode material for all solid-state lithium secondary batteries. *Electrochem. Commun.* **2007**, 9, 7, 1486-1490.
4. Takada, K.; Ohta, N.; Zhang, L.; Fukuda, K.; Sakaguchi, I.; Ma, R.; Osada, M.; Sasaki, T. Interfacial modification for high-power solid-state lithium batteries, *Solid State Ion.* **2008**, *179*, 1333.
5. Haruta, M.; Shiraki, S.; Suzuki, T.; Kumatani, A.; Ohsawa, T.; Takagi, Y.; Shimizu, R.; Hitosugi, T. Negligible "Negative Space-Charge Layer Effects" at Oxide-Electrolyte/Electrode Interfaces of Thin-Film Batteries. *Nano Lett.* **2015**, *15*, 3, 1498–1502.
6. Kobayashi, S.; Nishio, K.; Wilde, M.; Fukutani, K.; Shimizu, R.; Hitosugi, T. Protons inside the $LiCoO_2$ electrode largely increase electrolyte-electrode interface resistance in all-solid-state Li batteries. *J. Phys. Chem.* C, **2023**, *127*, 9, 4684–4688(2023).
7. Grahame, D. C. The Electrical Double Layer and the Theory of Electrocapillarity. *Chem. Rev.* **1947**, *41*, 441-501.
8. Sze, S. M., Physics of Semiconductor Devices (Wiley, New York, 2008)
9. T. Tsuchiya, Y. Oyama, S. Miyoshi, S. Yamaguchi. Nonstoichiometry-Induced Carrier Modification in Gapless Type Atomic Switch Device Using Cu_2S Mixed Conductor. Appl. Phys. Express 2 055002(2009)
10. T. Tsuchiya, S. Miyoshi, Y.Yamashita, H. Yoshikawa, K. Terabe, K. Kobayashi, S. Yamaguchi. Room temperature redox reaction by oxide ion migration at carbon/Gd-doped CeO2heterointerface probed by an in situ hard x-ray photoemission and soft x-ray absorption spectroscopies. Sci. Technol. Adv. Mater. 14, 045001(2013)
11. T. Tsuchiya, S. Miyoshi, Y. Yamashita, H. Yoshikawa, K. Terabe, K. Kobayashi, S. Yamaguchi. Direct observation of redox state modulation at carbon/amorphous tantalum oxide thin film hetero-interface probed by means of in situ hard X-ray photoemission spectroscopy. Solid State Ionics. 253, 110-118(2013)
12. Kawada, T. et al. Determination of oxygen vacancy concentration in a thin film of La0.6Sr0.4CoO3－δ by an electrochemical method. J. Electrochem. Soc. 149, E252 (2002).
13. T. Tsuchiya, M. Takayanagi, K. Mitsuishi, M. Imura, S. Ueda, Y. Koide, T. Higuchi, K. Terabe. The electric double layer effect and its strong suppression at Li+ solid

electrolyte/hydrogenated diamond interfaces. Commun. Chem. 4, 117 (2021) 117
14. M. Takayanagi, D. Nishioka, T. Tsuchiya, M. Imura, Y. Koide, T. Higuchi, K. Terabe. Ultrafast-switching of an all-solid-state electric double layer transistor with a porous yttria-stabilized zirconia proton conductor and the application to neuromorphic computing. Mater. Today Adv. 18, 100393(2023).
15. D. Nishioka, T. Tsuchiya, W. Namiki, M. Takayanagi, M. Imura, Y. Koide, T. Higuchi, K. Terabe. Edge-of-chaos learning achieved by ion-electron–coupled dynamics in an ion-gating reservoir. Sci. Adv. 8, eade1156 (2022)
16. Y. Yamaguchi, D. Nishioka, W. Namiki, T. Tsuchiya, M. Imura, Y. Koide, T. Higuchi, K. Terabe. Inverted input method for computing performance enhancement of the ion-gating reservoir. Appl. Phys. Express. 17, 024501(2024).
17. J. W. Liu, T. Teraji, B. Da, Y. Koide. Electrical property improvement for boron-doped diamond metal–oxide–semiconductor field-effect transistors. Appl. Phys. Lett. 124, 072103(2024)
18. J.W. Liu, T. Teraji, B. Da, Y. Koide. Suppression of High Threshold Voltage for Boron-Doped Diamond MOSFETs. IEEE Transactions on Electron Devices. 71, 1764-1768(2024)
19. Shao, Y., Maunders, C., Rossouw, D., Kolodiazhnyi, T. & Botton, G. A. Quantification of the Ti oxidation state in BaTi1－xNbxO3 compounds. Ultramicroscopy 110, 1014–1019 (2010).
20. M. Takayanagi, T. Tsuchiya, D. Nishioka, M. Imura, Y. Koide, T. Higuchi, K. Terabe. Accelerated/decelerated dynamics of the electric double layer at hydrogen-terminated diamond/Li^+ solid electrolyte interface. Mater. Today Phys. 31, 101006(2023)
21. S. Kim, H. J. Avila-Paredes, S. Wang, C.-T. Chen, R.A.D. Souza, M. Martin, Z. A. Munir, On the conduction pathway for protons in nanocrystalline yttria-stabilized zirconia, Phys. Chem. Chem. Phys. 11 (2009) 3035–3038.
22. M. Takayanagi, T. Tsuchiya, K. Kawamura, M. Minohara, K. Horiba, H. Kumigashira, T. Higuchi. Thickness-dependent surface proton conduction in (111) oriented yttria-stabilized zirconia thin film. Solid State Ion. 311, 46-51(2017)
23. M. Takayanagi, T. Tsuchiya, D. Nishioka, T. Higuchi, K. Terabe. Room temperature fabrication of highly proton conductive amorphous zirconia-based thin films achieved through precise nanostructure control. J. Mater. Chem. C. 11, 13311-13323(2023)
24. S. Miyoshi, Y. Akao, N. Kuwata, J. Kawamura, Y. Oyama, T. Yagi, S. Yamaguchi, Low-Temperature Protonic Conduction Based on Surface Protonics: An Example of Nanostructured Yttria-Doped Zirconia, Chem. Mater. 26 (2014) 5194–5200.
25. S. Miyoshi, Y. Akao, N. Kuwata, J. Kawamura, Y. Oyama, T. Yagi, S. Yamaguchi, Water

uptake and conduction property of nano-grained yttria-doped zirconia fabricated by ultra-high pressure compaction at room temperature, Solid State Ion. 207 (2012) 21–28.
26. R. Sato, S. Ohkuma, Y. Shibuta, F. Shimojo, S. Yamaguchi, Proton Migration on Hydrated Surface of Cubic ZrO2: Ab initio Molecular Dynamics Simulation, J. Phys. Chem. C. 119 (2015) 28925–28933.
27. T. Tsuchiya, K. Terabe, M. Aono. All-solid-state electric-double-layer transistor based on oxide ion migration in Gd-doped CeO2on SrTiO3single crystal. Appl. Phys. Lett. 103, 073110(2013)
28. T. Tsuchiya, M. Ochi, T. Higuchi, K. Terabe, M. Aono. Effect of Ionic Conductivity on Response Speed of SrTiO3-Based All-Solid-State Electric-Double-Layer Transistor. ACS Appl. Mater. Interf. 7, 12254-12260(2015)
29. Xu, K.; Islam, M. M.; Guzman, D.; Seabaugh, A. C.; Strachan, A.; Fullerton-Shirey, S. K. Pulse Dynamics of Electric Double Layer Formation on All-Solid-State Graphene Field-Effect Transistors. *ACS Appl. Mater. Interfaces* **2018**, *10* (49), 43166–43176.
30. He, Y.; Yang, Y.; Nie, S.; Liu, R.; Wan, Q. Electric-Double-Layer Transistors for Synaptic Devices and Neuromorphic Systems. *J. Mater. Chem. C* **2018**, *6* (20), 5336–5352.
31. Park, K.-W.; Cho, W.-J. Time-Dependent Sensitivity Tunable PH Sensors Based on the Organic-Inorganic Hybrid Electric-Double-Layer Transistor. *Int. J. Mol. Sci.* **2022**, *23* (18), 10842.
32. Zhu, J.; Yang, Y.; Jia, R.; Liang, Z.; Zhu, W.; Rehman, Z. U.; Bao, L.; Zhang, X.; Cai, Y.; Song, L.; Huang, R. Ion Gated Synaptic Transistors Based on 2D van Der Waals Crystals with Tunable Diffusive Dynamics. *Adv. Mater.* **2018**, *30* (21), 1800195.
33. R. Nakane, G. Tanaka, A. Hirose, Reservoir computing with spin waves excited in a garnet film. *IEEE access* **6**, 4462-4469 (2018).
34. R. Nakane, A. Hirose, G. Tanaka, Performance Enhancement of a Spin-wave-based Reservoir Computing System Utilizing Different Physical Conditions. Phys. Rev. Appl. 109 (2023) 034047.
35. G. Tanaka, T. Yamane, J. B. Héroux, R. Nakane, N. Kanazawa, S. Takeda, H. Numata, D. Nakano, A. Hirose, Recent advances in physical reservoir computing: A review. *Neural Netw.* **115**, 100-123 (2019).
36. J. Torrejon, M. Riou, F. A. Araujo, S. Tsunegi, G. Khalsa, D. Querlioz, P. Bortolotti, V. Cros, K. Yakushiji, A. Fukushima, H. Kubota, S. Yuasa, M. D. Stiles, Julie Grollier, Neuromorphic computing with nanoscale spintronic oscillators. *Nature* **547**, 428-431 (2017).
37. H. O. Sillin, R. Aguilera, H. H. Shieh, A. V. Avizienis, M. Aono, A. Z. Stieg, J. K. Gimzewski,A theoretical and experimental study of neuromorphic atomic switch

networks for reservoir computing. *Nanotechnology.* **24**,384004 (2013).
38. M. Akai-Kasaya, Y. Takeshima, S. Kan, K. Nakajima, T. Oya, T. Asai, Performance of reservoir computing in a random network of single-walled carbon nanotubes complexed with polyoxometalate. *Neuromorph. Comput. Eng.* **2**, 014003 (2022).
39. W. Jiang, L. Chen, K. Zhou, L. Li, Q. Fu, Y. Du, R. H. Liu, Physical reservoir computing using magnetic skyrmion memristor and spin torque nano-oscillator. *Appl. Phys. Lett.* **115**, 192403 (2019).
40. C. Du, F. Cai, M. A. Zidan, W. Ma, S. H. Lee, W. D. Lu, Reservoir computing using dynamic memristors for temporal information processing. *Nat. Commun.* **8**, 2204 (2017).
41. N. Akashi, T. Yamaguchi, S. Tsunegi, T. Taniguchi, M. Nishida, R. Sakurai, Y. Wakao, K. Nakajima, Input-driven bifurcations and information processing capacity in spintronics reservoirs. *Phys. Rev. Research* **2**, 043303 (2020).
42. J. Hochstetter, R. Zhu, A. Loeffler, A. D. Alvarez, T. Nakayama, Z. Kuncic, Avalanches and edge-of-chaos learning in neuromorphic nanowire networks. *Nat. Commun.* **12**, 4008 (2021).
43. J. Nakayama, K. Kanno, A. Uchida, Laser dynamical reservoir computing with consistency: an approach of a chaos mask signal. *Optics express* **24**, 8679-8692 (2016).
44. C. G. Langton, Computation at the edge of chaos: Phase transitions and emergent computation. *Physica D: nonlinear phenomena* **42**, 12-37 (1990).
45. D. Nishioka, Y. Shingaya, T. Tsuchiya, T. Higuchi, K. Terabe. Few- and single-molecule reservoir computing experimentally demonstrated with surface-enhanced Raman scattering and ion gating. Sci. Adv. 10, eadk6438(2024)
46. T. Wada, D. Nishioka, W. Namiki, T. Tsuchiya, T. Higuchi, K. Terabe. A Redox-Based Ion-Gating Reservoir, Utilizing Double Reservoir States in Drain and Gate Nonlinear Responses. Adv. Intell. Syst. 5, 2300123(2023)
47. D. Nishioka, T. Tsuchiya, T. Higuchi, K. Terabe. Enhanced synaptic characteristics of H_xWO_3-based neuromorphic devices, achieved by current pulse control, for artificial neural networks. Neuromorphic Computing and Engineering. 3, 034008(2023)
48. S. Mallik, T. Tsuruoka, T. Tsuchiya, K. Terabe. Effects of Mg Doping to a LiCoO2 Channel on the Synaptic Plasticity of Li Ion-Gated Transistors. ACS Appl. Mater. Interf. 15, 47184-47195(2023)
49. K. Shibata, D. Nishioka, W. Namiki, T. Tsuchiya, T. Higuchi, K. Terabe. Redox-based ion-gating reservoir consisting of (104) oriented $LiCoO_2$ film, assisted by physical masking. Sci. Rep. 13,21060(2023)
50. W. Namiki, D. Nishioka, T. Tsuchiya, T. Higuchi, K. Terabe. Magnetization Vector Rotation Reservoir Computing Operated by Redox Mechanism. Nano Lett. 24, 4383-

4392(2024)
51. Y. Isoda, D. Kan, Y. Ogura, T. Majima, T. Tsuchiya, Y. Shimakawa. Electrochemical control and protonation of the strontium iron oxide SrFeOy by using proton-conducting electrolyte. Appl. Phys. Lett. 120, 091601(2022)
52. Y. Isoda, D. Kan, T. Majima, Y. Shimakawa. Orientation-dependent electrochemical reduction and proton evolution in the oxygen-deficient perovskite SrFeO2.5+y. Appl. Phys. Express. 16,015506(2023).
53. Xie, L., Isoda, Y., Majima, T. et al. Orientation-dependent electrochemical response of LaSrNiO4 epitaxial films. J Solid State Electrochem (2023). https://doi.org/10.1007/s10008-023-05759-5
54. H. Zhang, T. Tsuchiya, C. Liang, K. Terabe. Size-Controlled AgI/Ag Heteronanowires in Highly Ordered Alumina Membranes: Superionic Phase Stabilization and Conductivity. Nano Lett. 15, 5161-5167(2015)
55. T. Tsuchiya, M. Imura, Y. Koide, K. Terabe. Magnetic Control of Magneto-Electrochemical Cell and Electric Double Layer Transistor. Scientific Reports. 7 [1] (2017) 10.1038/s41598-017-11114-2
56. T. Tsuchiya, K. Terabe, R. Yang, M. Aono. Nanoionic devices: Interface nanoarchitechtonics for physical property tuning and enhancement. Japanese Journal of Applied Physics. 55 [11] (2016) 1102A4
57. K. Terabe, T. Tsuchiya, R. Yang, M. Aono. Nanoionic devices enabling a multitude of new features. Nanoscale. 8,13873-13879(2016)
58. D.Y. Kim, S. Miyoshi, T. Tsuchiya, S. Yamaguchi. Defect chemistry and electrochemical properties of BaZrO3 heavily doped with Fe. ECS Transactions, 45, 1, 161 – 170(2012)
59. T. Tsuchiya, T. Nakayama, K. Ariga. Nanoarchitectonics Intelligence with atomic switch and neuromorphic network system. Appl. Phys. Express. 15, 100101(2022).
60. K. Ariga. Nanoarchitectonics: the method for everything in materials science. Bull. Chem. Soc. Jpn. 97, 1, uoad001(2023).